Catalysis Today 144 (2009) 172–176

Contents lists available at ScienceDirect

Catalysis Today

journal homepage: www.elsevier.com/locate/cattod

Influence of solution chemistry on the properties of hydrothermally grown TiO_2 for advanced applications

D. Vernardou [a,b,c,*], K. Vlachou [c], E. Spanakis [b,c,d], E. Stratakis [c,d,e], N. Katsarakis [a,b,d], E. Kymakis [a,e], E. Koudoumas [a,e]

[a] School of Applied Technology, Technological Educational Institute of Crete, 710 04 Heraklion, Crete, Greece
[b] Science Department, School of Applied Technology, Technological Educational Institute of Crete, 710 04 Heraklion, Crete, Greece
[c] Department of Materials Science and Technology, University of Crete, 710 03 Heraklion, Crete, Greece
[d] Institute of Electronic Structure and Laser, Foundation for Research & Technology-Hellas, P.O. Box 1527, Vassilika Vouton, 711 10 Heraklion, Crete, Greece
[e] Electrical Engineering Department, Technological Educational Institute of Crete, 710 04 Heraklion, Crete, Greece

ARTICLE INFO

Article history:
Available online 19 March 2009

Keywords:
Hydrothermal growth
Solution chemistry
Anatase TiO_2
Sodium titanate
Photoinduced properties

ABSTRACT

It is demonstrated that the properties of hydrothermally deposited titanium (IV) oxide (TiO_2) films are greatly affected by the solution chemistry. Anatase TiO_2 films grown using i-PrOH presented the best reversible photoinduced hydrophilic response, reaching a contact angle (CA) of 15° and 83% photocatalytic activity as well as measurable photoconductivity. Inclusion of as low as 0.02 M NaOH in the solution resulted in films probably consisted of sodium titanate exhibiting good photoinduced properties, which makes it a promising candidate for various applications. In contrast, rutile TiO_2 films prepared using EtOH as a solvent showed weak photoinduced activity. The correlation of solution chemistry with the morphology and the photoinduced properties of the materials are discussed.

1. Introduction

Titanium (IV) oxide (TiO_2) or titania is one of the most promising semiconductors for applications in various technologies such as solar cells [1] photocatalysis [2], anti-fogging and self-cleaning or anti-bacterial coatings [3] having the added advantage of being a non-toxic and low-cost material [4]. The photoinduced properties involved in these applications can be regulated by controlling the TiO_2 crystallographic structure and morphology [5]. In addition, transparent conducting applications can already be realised for TiO_2 by doping with Nb [6].

Anatase and rutile TiO_2 have been widely studied as photocatalysts [7], anatase exhibiting a higher activity than rutile due to its particular band structure [8]. Furthermore, surface roughness is an important parameter for the photocatalytic activity of this material [5]. Photocatalysis takes place on the surface of the film under the presence of adsorbed water molecules. The wider is the exposed surface of the films the higher is expected to be the number of photocatalytic events. The efficiency of the effect per unit of film area will thus be enhanced by a corresponding increase of the ratio of the actual surface of the films to the deposited area. Such an increase is the natural consequence of surface roughness.

TiO_2 with such properties can be developed using several techniques such as sputtering [9], chemical vapour deposition (CVD) [10], hydrolysis [11], sol–gel methods [12] and hydrothermal synthesis [13–15], most of them requiring costly equipment and/or vacuum and/or high temperatures and/or hazardous chemicals. Hydrothermal synthesis is a "one pot" process, requiring non-hazardous chemicals, low temperatures and atmospheric pressure. Moreover, it can be expanded to large substrates with the only shortcoming being the long preparation times needed for full coverage. Finally, with this method, the structural and morphological characteristics of the samples can be tailored by simply controlling the solution chemistry (precipitation/dispersion conditions affecting the thermodynamic stabilization of the system) [16]. Therefore, hydrothermal synthesis seems to be a rather attractive technique for the deposition of TiO_2.

The aim of the present work is to provide insight on the correlation of solution chemistry with morphology and photoinduced properties of hydrothermally grown titanium oxide, at 95 °C on Corning 7059 substrates. It is noteworthy that under appropriate conditions, it is possible to grow sodium titanate with good reversible photoinduced hydrophilic and photocatalytic activity.

* Corresponding author. Tel.: +30 2810379845.
E-mail address: dimitra@iesl.forth.gr (D. Vernardou).

0920-5861/$ – see front matter © 2009 Elsevier B.V. All rights reserved.
doi:10.1016/j.cattod.2009.02.009

2. Experimental

The growth of titanium oxide on Corning 7059 was performed by the hydrothermal method using as precursors three different solutions: (series 1) TTIP ($Ti[(OCH(CH_3)_2)]_4$), propanol (i-PrOH, $(CH_3)_2CHOH$)) and MilliQ water, (series 2) TTIP, ethanol (EtOH, CH_3CH_2OH) and MilliQ water and (series 3) TTIP, i-PrOH, MilliQ water and 0.02 M NaOH/i-PrOH solution. For growth using i-PrOH as solvent, the solution preparation involved initially the stirring of 12 M i-PrOH with 0.1 M MilliQ H_2O, followed by the addition of 0.03 M TTIP. For growth using EtOH, the solution preparation involved the same procedure as for series 1 but instead of i-PrOH, EtOH was used. Finally, for growth using 0.02 M NaOH/i-PrOH, the procedure is the same as in series 1 with the further addition of 10 ml, 0.02 M NaOH/i-PrOH under continuous stirring. In each case, the solution was placed in a Pyrex glass bottle with polypropylene autoclavable screw cap, with the substrate positioned on the bottom, and was heated at 95 °C for deposition periods of 20 h, 30 h, 40 h and 50 h in a regular laboratory oven. After deposition, the samples were thoroughly washed with the respective solvent (i-PrOH or EtOH), in order to eliminate residual salts, and dried in air at 95 °C.

X-ray diffraction (XRD) measurements were performed using the Cu Kα line of a Rigaku (RINT 2000) Diffractometer. Raman measurements were carried out in the 100–700 cm^{-1} wavenumber range using the 473 nm excitation of a Nicolet Almega XR micro-Raman Spectrometer. UV–vis transmittance measurements were performed with a PerkinElmer Lambda 950 spectrometer over the wavelength range of 250–1000 nm. Surface imaging was carried out on an atomic force microscope (AFM) in tapping mode (Digital Instruments–Nanoscope IIIa) using Si cantilevers. Contact angle (CA) measurements were performed by positioning a 10 μL distilled, deionised Millipore water droplet on the surface of the samples. Images of the droplet were captured by a CCD camera and the CA was subsequently determined by applying an image-processing algorithm. Photoinduced hydrophilicity was evaluated by irradiating the samples with 4 mW cm^{-2} UV light of a Hg lamp, centred at 365 nm, for predetermined periods of time, at ambient conditions. The same lamp was used to acquire photoconductivity measurements from the ohmic part of corresponding current–voltage (*I–V*) curves of samples having sputter-deposited gold contacts separated by 2.5 mm. Finally, the photocatalytic activity of the samples was assessed utilising a stearic acid test. At first the samples were coated with stearic acid by spin coating a 30 μL droplet of stearic acid diluted in chloroform (0.1 M solution) and subsequent drying at 80 °C in air for 10 min. The test was performed by recording the reduction of the IR absorbance of the C–H stretching band of stearic acid (2800–3000 cm^{-1}), under UV illumination, after certain time intervals. IR absorbance was recorded with a Fourier transform infrared spectrometer (FTIR) (IRPRESTIGE-21, Shimadzu), in transmission mode and UV illumination was provided by a black light blue lamp centred at 365 nm and having a power density of 2 mW cm^{-2}. Each characterization method was conducted on at least three samples prepared under the same conditions for consistency and reproducibility.

3. Results and discussion

Since growth times shorter than 20 h resulted in TiO_2 films with no photoinduced response, a range of deposition periods 20–50 h was chosen for our studies. Propanol was selected based on considerations of similar procedures reported in the literature [17,18], while ethanol was used for the control of the morphological characteristics of the films via the alteration of precipitation rate of the solution [19]. Regarding the choice of using sodium hydroxide in these experiments, this was based on experiments reported in the literature, indicating that in such a way, the size and the shape of the nanoparticles can be controlled [20,21] (resulting in an increase surface to volume ratio) and the photocatalytic activity of the films can be enhanced [22]. The sodium hydroxide solutions were prepared in i-PrOH since water accelerates precipitation, which in turn inhibits deposition of enough material. Furthermore, NaOH concentrations higher than 0.02 M resulted in powdery films, since no coherent hydrothermal growth occurred. Thus, the NaOH concentration had a significant influence on the solution and the consequent growth chemistry, occurring at the substrate surface. Our results indicated that control of the precipitation rate of the solution and the deposition of coherent films can be achieved for NaOH concentration around 0.02 M. All grown samples passed the Scotch tape test (removal of an X shaped piece of sticking tape) [23] and were stable in air for

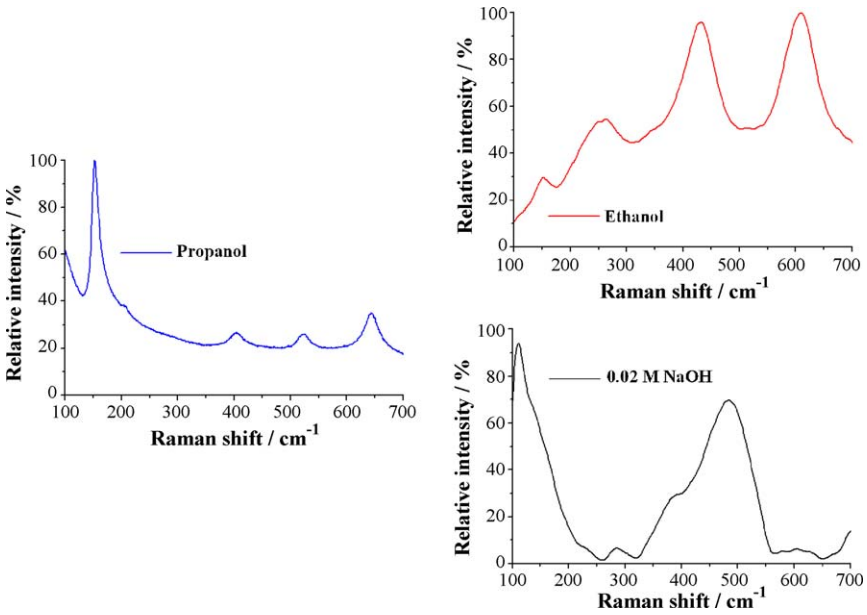

Fig. 1. Raman spectra of the grown films on Corning 7059 for a deposition time of 50 h using i-PrOH, EtOH and 0.02 M NaOH/i-PrOH.

over six months. They all presented a flat transmission spectrum in the visible range. Transmission always decreased with deposition time reaching a lowest value of 70% among the samples of this study, which is satisfactory for simple or conductive transparent window applications.

XRD patterns of the as-deposited films showed no evidence of diffraction peaks, indicating that the films were largely amorphous. On the other hand, Raman spectroscopy indicated the growth of well-defined phases. Fig. 1 shows the Raman spectra of the as-deposited films grown on Corning 7059 for deposition time of 50 h. For the samples grown using i-PrOH, anatase TiO_2 was obtained, with respective phonon frequencies: 144 cm^{-1} (E_g), 398 cm^{-1} (B_{1g}), 516 cm^{-1} (A_{1g}) and 638 cm^{-1} (E_g) [24], while for those grown using EtOH, rutile TiO_2 was present, with respective phonon frequencies: 146 cm^{-1} (B_{1g}), 443 cm^{-1} (E_g) and 609 cm^{-1} (A_{1g}). In addition, for the rutile case, there was a second-order scattering feature at 243 cm^{-1} [25]. The samples deposited using the 0.02 M NaOH/i-PrOH solution gave Raman spectra that indicated the presence of $Na_2Ti_3O_7$ [26]. Moreover, it was observed in series 1 and 2 that for lower deposition periods, the peaks are broader and lower in intensity, indicating anatase and rutile TiO_2 of enhanced crystalline quality for higher growth periods. For series 3, the peaks corresponding to sodium titanate are broad for the whole range of deposition periods, indicating possibly either the suppressed crystalline quality of sodium titanate or the co-existence of anatase [24] or rutile TiO_2 [25] with the sodium titanate phase [26].

In terms of film crystallinity, X-ray diffraction analysis of all deposited films showed no evidence of diffraction peaks. XRD is however known to probe the long range order crystallinity of materials, while Raman is a probe of the influence of even localized short-range order to the vibrational modes of bond configurations [27]. Therefore, the simultaneous presence of well identified Raman signatures with the absence of XRD peaks in our films suggests that they are mainly amorphous retaining however a short range, within a few neighboring atoms, crystalline ordering. The important outcome of these results is that a perfect crystalline structure is not necessary for photoinduced properties to occur as noted below; the presence of localized short range order is, on the contrary, adequate. In addition, the phase of hydrothermally grown TiO_2 films can be controlled solely by modifying the solution chemistry while keeping all other deposition conditions constant.

Turning now to surface morphology, Fig. 2 presents high resolution AFM images of the as-deposited samples grown using EtOH and 0.02 M NaOH/i-PrOH for a deposition period of 20 h at 95 °C. For the sample grown using EtOH (Fig. 2 (a)), the image indicates the formation of fine agglomerations consisting of nanoparticles with non-uniform size around 20 nm. For longer deposition times, the agglomerations were found to be less pronounced, the nanoparticles simultaneously becoming larger, approaching 40 nm approximately. Similar behavior was observed for the films grown using i-PrOH. Furthermore, for the thin films deposited using 0.02 M NaOH/i-PrOH (Fig. 2 (b)), spherical nanoparticles are observed with almost uniform size and homogeneous distribution. For longer deposition times, the size of the nanoparticles was observed to get smaller, their distribution becoming less uniform. The roughness of the sample grown using i-PrOH was determined to attain a value of 4.4 nm while that for the case of EtOH was only 1.8 nm, for the same deposition period of 20 h. Regarding the sample grown using the 0.02 M NaOH/i-PrOH solution, the surface roughness was much larger, approaching a value of 20 nm. This was a very important result since the increased roughness can enhance the adsorption of water molecules, resulting in an increased photocatalytic response [5].

Fig. 3 presents the variation of the roughness of the TiO_2 films as a function of the deposition period. As shown, with increasing

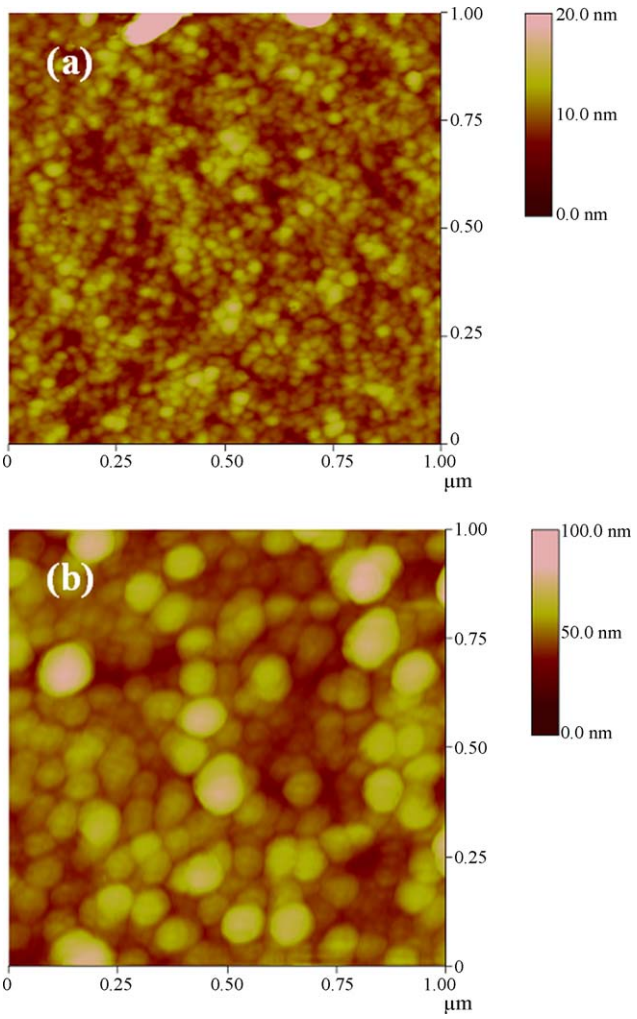

Fig. 2. AFM images of the films deposited using EtOH (a) and 0.02 M NaOH/i-PrOH (b) on Corning 7059 for a deposition time of 20 h at 95 °C.

deposition time, the roughness of the films increases for samples grown using i-PrOH, while it remains almost constant for the case of EtOH. In contrast, the roughness was found to decrease with increasing growth time for the case of the samples grown using the 0.02 M NaOH/i-PrOH solution. In addition, it was noticed that the shape of the nanostructures for the samples grown using NaOH/i-PrOH does not change significantly to nanowires or nanotubes, as

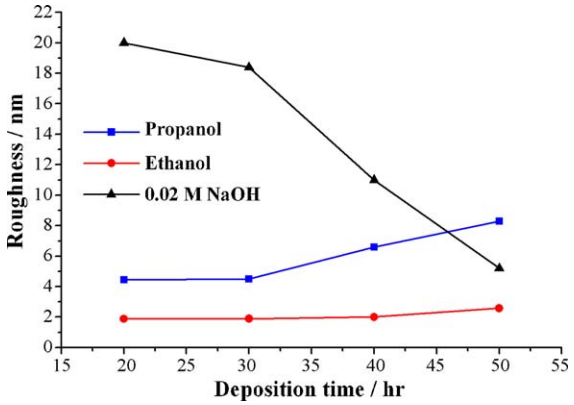

Fig. 3. Roughness (1 × 1 μm) dependence on deposition time for titanium oxide samples grown using i-PrOH, EtOH and 0.02 M NaOH/i-PrOH on Corning 7059 glass substrate at 95 °C.

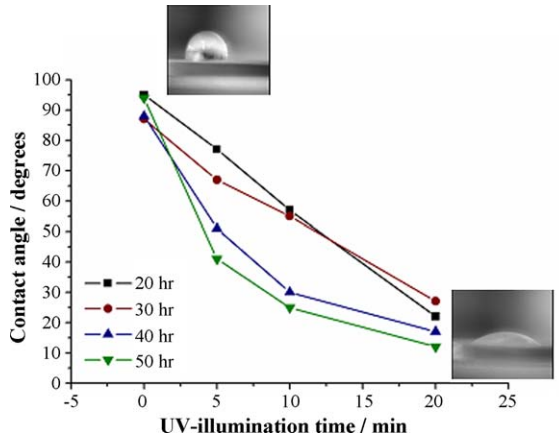

Fig. 4. Water contact angle dependence on UV illumination time using 4 mW cm^{-2} UV light of a Hg lamp, in atmospheric air and temperature of 25 °C of samples grown using i-PrOH for a range of deposition periods 20–50 h.

reported in the literature [20,21], because in our case, NaOH is only a part of the solution and not the solvent. However, the presence of sodium was observed to increase the roughness, which is in agreement with the literature [22].

Fig. 4 shows the variation of water contact angle for anatase TiO_2 films grown using i-PrOH, as a function of the exposure time to UV radiation. The CA of all as-deposited films before UV illumination was determined to be in the range of 85–95°. Moreover, the change in the CA after illumination was found to depend on the growth time, the most efficient photoinduced activity exhibited by the samples grown for the largest deposition periods (a change of 75° in the CA for the 50 h sample). Therefore, the photoactivity of the TiO_2 films is improved with increasing growth time, a behavior which is consistent with the sharper and more intense peaks in Raman spectra (Fig. 1) and the enlargement of the surface roughness (Fig. 3). The CA was observed to return to its initial value after storing the samples in dark at room temperature for seven days.

Fig. 5 shows the variation of CA for the samples grown using 0.02 M NaOH/i-PrOH as a function of the exposure time to UV radiation. The contact angle of these as-deposited films was measured to be in the range of 70–85° before UV light illumination. Analysis of the behaviour of these films showed that short deposition time results in better photoactivity, the best response observed for samples grown for a deposition period of 20 h, where the contact angle varied from 75 to 15°. The contact angle was observed to return, as well, to its initial value after storing the

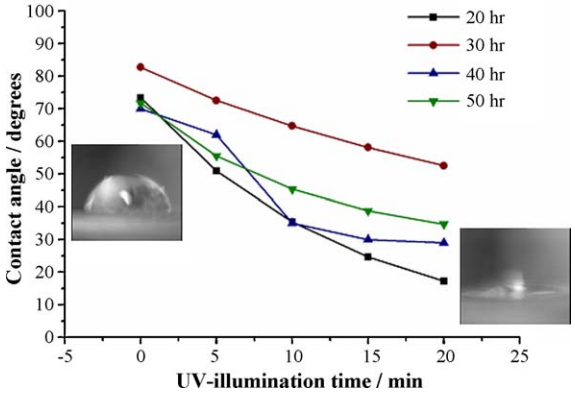

Fig. 5. Water contact angle dependence on UV illumination time using 4 mW cm^{-2} UV light of a Hg lamp, in atmospheric air and temperature of 25 °C for samples grown using 0.02 M NaOH/i-PrOH for a range of deposition periods 20–50 h.

samples in dark for seven days at room temperature. It is interesting to note that short deposition times was also found to result in higher surface roughness, the sharpness or the intensity of the Raman peaks remaining unaffected by the deposition time. Therefore, it seems plausible to suggest that the most important factor affecting the photoinduced change of the wetting response of our TiO_2 samples is the surface roughness.

Regarding the TiO_2 samples grown using EtOH, no photo-induced change in the water contact angle was observed in all cases after 20 min exposure to UV radiation. Rutile is not known to present photoinduced hydrophilic response as anatase is, based on the literature [28]. The origin of this difference might be similar to that of their different photocatalytic response, which however, needs further investigation for a better understanding of the corresponding mechanisms.

A measure of photocatalytic activity that is commonly used for the films is the degradation rate of stearic acid [29,30]. Fig. 6 clearly demonstrates that anatase TiO_2 samples grown using i-PrOH for a deposition time of 20 h present the most efficient photocatalytic activity, degrading stearic acid by almost 83%. This behaviour may be attributed to the small size of the nanoparticles, which increases their surface to volume ratio. In contrast, the stearic acid was not appreciably degraded (26%) for the samples grown using EtOH, which could arise from the presence of rutile and the smooth surface of the samples (Fig. 2). Regarding the material grown using 0.02 M NaOH/i-PrOH, the best photocatalytic activity (51%) was also demonstrated for a deposition time of 20 h, the enhanced response attributed to the higher surface roughness, which consequently promotes the adsorption of water molecules [5]. Further studies are in progress for the better understanding of the observed behaviour.

Regarding other reported results about the photocatalytic response of TiO_2, titania prepared by sol–gel presented photo-catalytic activity of 100% after approximately 35 min under 30 W m^{-2} UV lamp irradiation [30], which is slightly higher intensity than the one used in this work. Furthermore, titania grown by CVD showed 100% degradation activity after 5000 min [29], which is longer period in comparison with our films. We therefore note that in terms of stearic acid degradation, the hydrothermally grown films produced in this work are of comparable efficiency to crystalline films grown by other techniques.

Finally, Fig. 7 shows representative current–voltage (I–V) curves taken in the dark and under UV illumination for the

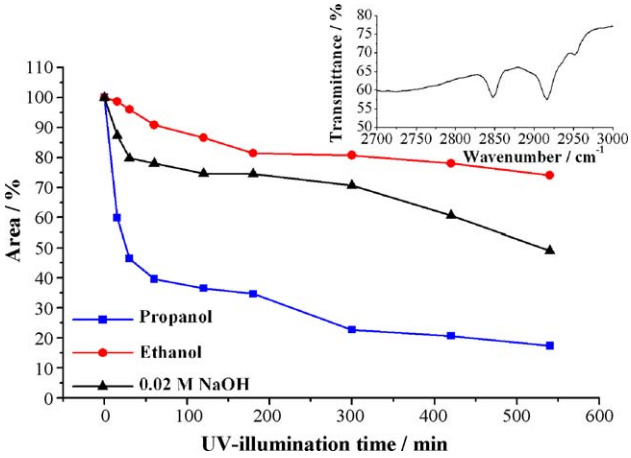

Fig. 6. Variation of the area under the C–H stretching region of the stearic acid spectrum (inset) as a function of the UV illumination time with 2 mW cm^{-2} UV light in atmospheric air and a temperature of 25 °C for thin films grown using i-PrOH, EtOH and 0.02 M NaOH/i-PrOH for deposition period of 20 h.

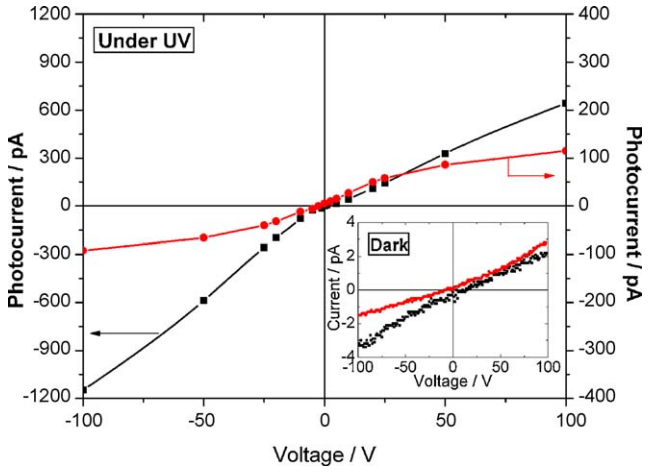

Fig. 7. Current–voltage (*I–V*) curves taken in ambient conditions, in the dark and under 4 mW cm^{-2} UV illumination for the samples grown for 20 h from TTIP in an EtOH (solid squares) and in an i-PrOH/NaOH (solid circles) solution.

samples grown for 20 h using EtOH and NaOH/i-PrOH as a solvent, the samples grown using i-PrOH exhibiting similar behavior as those from NaOH/i-PrOH. I–V curves, taken for all samples in the dark show good ohmic behaviour for the entire voltage range of −100 V–100 V utilized, revealing that gold is appropriate for providing ohmic contacts to these materials. Photo-activated curves show either ohmic behaviour (as is the case for the 20 h EtOH sample of Fig. 7) or ohmic to subohmic transitions (as is the case for the 20 h NaOH/i-PrOH sample of Fig. 7). Such transitions are observed also in other amorphous materials and are attributed to positive space charge accumulated near the cathode [31] due to the drift length, i.e. mobility, discrepancy between photogenerated electrons and holes [32]. In such cases the photoconductivity is calculated from the low-voltage, ohmic part of the I–V curves. The photoresponse [33] of titanium oxide prepared with i-PrOH and NaOH/i-PrOH, defined as the ratio of the photo to dark conductivity, was found to range around 100 and to be three times lower than that of the material prepared with EtOH. Degraded conductivity is commonly attributed to adsorbed oxygen molecules that reduce to O_2^- by removing electrons from the conduction band [34]. The loss of photogenerated electron–hole pair concentrations found for the PrOH-prepared samples, compared to the EtOH ones, could be due to a larger proportion of those carriers being trapped at the surface of the former materials. Such surface trapped carriers are responsible for the production of hydroxyl radicals that fuel the photocatalytic ability of the films [35]. The above reasoning seems plausible as it renders the degraded photoresponse of i-PrOH and NaOH/i-PrOH prepared titanium oxide films compatible to their pronounced photocatalytic efficiency.

Therefore, we have experimentally demonstrated that TiO_2 samples grown using i-PrOH for a deposition period of 20 h exhibits the best reversible photoinduced hydrophilic and photocatalytic activity among all grown samples, possibly due to the presence of anatase and the small size of the nanoparticles that enhances their actual surface to deposited area ratio. Moreover, we have shown that films with sodium titanate inclusions, grown under certain conditions, present quite efficient photoinduced properties possibly due to the increased number of photoactive sites (higher surface roughness) [5].

4. Conclusion

The results presented in this paper reveal that under suitable deposition conditions, it is possible to control the phase of hydrothermally grown titanium oxide thin films. Depending on the solution chemistry, Raman analysis indicated that the formation of anatase, rutile or $Na_2Ti_3O_7$ is possible, the corresponding photo-induced properties strongly depending on the phase of the film. Anatase films grown for a deposition period of 20 h using i-PrOH were found to simultaneously exhibit optimum photoinduced reversible hydrophilic and photocatalytic response as well as measurable photoconductivity. In contrast, the photoresponse of rutile films grown using EtOH was found to be quite weak. Finally, it was shown that sodium titanate may be deposited at 95 °C, exhibiting quite efficient photoinduced properties.

Acknowledgements

This work was co financed by 75% from the European Regional Development Fund and by 25% from national Greek resources (INTERREG IIIA Greece-Cyprus).

References

[1] O. Zywitzki, T. Modes, P. Frach, D. Glöss, Surf. Coat. Technol. 202 (2008) 2488.
[2] B. O'Regan, M. Grätzel, Nature 353 (1991) 737.
[3] T. Carlson, G.L. Giffin, J. Phys. Chem. 90 (1986) 5896.
[4] R. Wang, K. Hashimoto, A. Fujishima, Nature 388 (1997) 431.
[5] T. Gerfin, M. Grätzel, L. Walder, in: K.D. Karlin (Ed.), Molecular and Supermolecular Surface Modification of Nanocrystalline TiO_2 Films: Charge Separating and Charge Injecting Devices, John Wiley & Sons Inc., New York, 1997.
[6] Y. Furubayashi, T. Hitosugi, Y. Yamamoto, K. Inaba, G. Kinoda, Y. Hirose, T. Shimada, T. Hasegawa, Appl. Phys. Lett. 86 (2005) 252101.
[7] Z. Ambrus, K. Mogyorósi, A. Szalai, T. Alapi, K. Demeter, A. Dombi, P. Sipos, Appl. Catal. A 340 (2008) 153.
[8] A. Fujishima, K. Hashimoto, T. Watanabe, TiO_2 Photocatalysis – Fundamentals and Applications, BKC, Tokyo, 1999.
[9] L. Miao, P. Jin, K. Kaneko, A. Terai, N. Nabatova-Gabain, S. Tanemura, Appl. Surf. Sci. 212–213 (2003) 255.
[10] S.K. Pradhan, P.J. Reucroft, F. Yang, A. Dozier, J. Cryst. Growth 256 (2003) 83.
[11] K.D. Kim, H.T. Kim, Powder Technol. 119 (2001) 164.
[12] T. Sugimoto, K. Okada, H. Itoh, J. Colloid Interface Sci. 193 (1997) 140.
[13] M. Wu, G. Lin, D. Chen, G. Wang, D. He, S. Feng, R. Xu, Chem. Mater. 14 (2002) 1974.
[14] S. Yang, L. Gao, J. Am. Ceram. Soc. 88 (2005) 968.
[15] H.Y. Zhu, Y. Lan, X.P. Gao, S.P. Ringer, Z.F. Zheng, D.Y. Song, J.C. Zhao, J. Am. Chem. Soc. 127 (2005) 6730.
[16] K. Byrappa, M. Yoshimura, Handbook of Hydrothermal Technology, William Andrew Publishing, New York, 2001.
[17] M.C. Carotta, S. Gherardi, C. Malagu, M. Nagliati, B. Vendemiati, G. Martinelli, M. Sacerdoti, I.G. Lesci, Thin Solid Films 515 (2007) 8339.
[18] C. Su, C.-M. Tseng, L.-F. Chen, B.-H. You, B.-C. Hsu, S.-S. Chen, Thin Solid Films 498 (2006) 259.
[19] Y. Takahashi, Y. Matsuoka, J. Mater. Sci. 23 (1988) 2259.
[20] Z.-Y. Yuan, B.-L. Su, Colloid Surf. A: Physicochem. Eng. Aspects 241 (2004) 173.
[21] T. Kasuga, M. Hiramatsu, A. Hoson, T. Sekino, K. Niihara, Adv. Mater. 1307 (1999) 11.
[22] C.-K. Lee, C.-C. Wang, M.-D. Lyu, L.-C. Juang, S.-S. Liu, S.-H. Hung, J. Colloid Interf. Sci. 316 (2007) 562.
[23] T.D. Manning, I.P. Parkin, R.J.H. Clark, D. Sheel, M.E. Pemble, D. Vernardou, J. Mater. Chem. 12 (2002) 2936.
[24] Y. Lei, L.D. Zhang, J.C. Fan, Chem. Phys. Lett. 338 (2001) 231.
[25] V. Swamy, B.C. Muddle, Q. Dai, Appl. Phys. Lett. 89 (2006) 163118.
[26] C.E. Bamberger, G.M. Begun, J. Am. Ceram. Soc. 70 (3) (1987) C–48.
[27] M. Ocana, J.V. Garcia, C.J. Serna, J. Am. Ceram. Soc. 75 (1992) 2010.
[28] J.C. Yu, J. Yu, W. Ho, J. Zhao, J. Photochem. Photobiol. A: Chem. 148 (2002) 331.
[29] A. Mills, N. Elliott, I.P. Parkin, S.A. O'Neill, R.J. Clark, J. Photochem. Photobiol. A: Chem. 151 (2002) 171.
[30] M.E. Simonsen, H. Jensen, Z. Li, E.G. Søgaard, J. Photochem. Photobiol. A: Chem. (2008), doi:10.1016/j.jphotochem.2008.07.013.
[31] E. Spanakis, E. Stratakis, N. Kopidakis, P. Tzanetakis, H. Fritzsche, J. Non-Cryst. Solids 266–269 (2000) 247.
[32] V. Yu Timoshenko, V. Duzhko, Th. Dittrich, Phys. Status Solidi A 182 (2000) 227.
[33] A.E. Jimenez Gonzalez, S. Gelover Santiago, Semicond. Sci. Technol. 22 (2007) 709.
[34] K. Pomoni, A. Vomvas, Chr. Trapalis, Thin Solid Films 479 (2005) 160.
[35] N. Sakai, A. Fujishima, T. Watanabe, K. Hashimoto, J. Phys. Chem. B 105 (2001) 3023.